

## MODELING THE KINETICS OF HYDROXYAPATITE CATALYZED TRANSESTERIFICATION REACTION

Dr. Ali A. Jazie Al-Khaledy

Department of Chemical Engineering, College of Engineering, University of Al-Qadisiya, Addywania, Iraq

[jazieengineer@yahoo.com](mailto:jazieengineer@yahoo.com)

Received 1 April 2014

Accepted 25 November 2014

### ABSTRACT

A bone waste was utilized as a cost effective catalyst for the transesterification of Indian mustard oil. This high efficient and low-cost waste catalyst could make the biodiesel production from Indian mustard oil competitive with petroleum diesel. The catalysts samples were calcined at different temperatures (800°C, 900°C and 1000°C) for 2 hrs. The samples were characterized by using X-Ray diffraction (XRD), Fourier transform infrared spectroscopy (FTIR) and BET surface area analyzer. A simple model was used to study the kinetics of hydroxyapatite-catalyzed transesterification of mustard oil. The optimum conditions for biodiesel production were (reaction temperature (60°C), a methanol-to-oil molar ratio (20:1) and catalyst amounts (18% based on oil weight). Two steps were concluded for the transesterification process, the initial one is the triglyceride (TG) mass transfer controlled region, The second one is the chemical reaction controlled region. The high adsorbed methanol concentration and the lower availability of active specific catalyst surface caused the TG mass transfer controlled region. Increasing the catalyst amount in the transesterification process caused increasing both the TG mass transfer and chemical reaction rates. The effect of mixing conditions in the transesterification process was predicted in the modeling strategy.

**Keywords:** Modeling, Kinetics, Mustard oil, Transesterification, Hydroxyapatite.

### NOMENCLATURE

$a_m$	specific surface of catalyst ( $m^2/g$ )
$C_A$	concentration of TG in the liquid phase ( $mol/dm^3$ )
$C_{A0}$	initial concentration of TG in the liquid phase ( $mol/dm^3$ )
$C_{A,s}$	concentration of TG on the interfacial solid liquid area ( $mol/dm^3$ )
$C_B$	concentration of methanol in the liquid phase ( $mol/dm^3$ )
$C_R$	concentration of FAME in the liquid phase ( $mol/dm^3$ )
$C$	integration constant (1)
$d_p$	catalyst particle size (m)
$D$	molecular diffusion coefficient ( $m^2/s$ )
$D_{eff}$	effective diffusion coefficient ( $m^2/s$ )
$k$	pseudo-first order reaction rate constant ( $min^{-1}$ )
$k_{ad}$	methanol adsorption rate constant ( $min^{-1}$ )
$k_{app}$	apparent process rate constant ( $min^{-1}$ )

$k_{s,A}$	TG mass transfer coefficient towards catalyst surface activesites (m/min)
$k_{mt,A}$	volumetric TG mass transfer coefficient towards the catalystsurface ( $=k_{s,A} \cdot h \cdot a_m \cdot m_{HAP}/V$ )( $\text{min}^{-1}$ )
$m_{HAP}$	mass of heterogeneous catalyst (g)
$Q$	the instantaneous concentration of adsorbed methanol(mol/g)
$Q_{max}$	the maximal concentration of adsorbed methanol (mol/g)
$(-r_A)$	rate of TG consumption, (mol/( $\text{dm}^3 \text{ min}$ ))
$(-r_B)$	rate of methanol consumption (mol/( $\text{dm}^3 \text{ min}$ ))
$R_p$	catalyst particle radius (m)
$T$	time (min)
$TG$	content of TG in the FAME/oil fraction of the reactionmixture (%)
$Th$	Thiele modulus (l)
$V$	volume of the reaction mixture volume ( $\text{cm}^3$ )
$x_A$	degree of TG conversion (l)
<b>Greek symbols</b>	
$\varepsilon_p$	catalyst particle porosity (l)
$\varepsilon_p$	catalyst particle tortuosity (l)
$\theta$	fraction of the catalyst available active specific surface(l)
$\theta_o$	fraction of the catalyst available active specific surfacein the initial phase of the transesterification process (l)
<b>Abbreviations</b>	
<b>TG</b>	triglycerides
<b>DG</b>	diglycerides
<b>MG</b>	monoglycerides
<b>FAME</b>	fatty acid methyl esters
<b>HAP</b>	hydroxyapatite catalyst

## نمذجة حركية تفاعل الترانساسترة المحفزة بواسطة الهيدروكسي اباتايت

### الخلاصة

مخلفات العظام استخدمت كعامل مساعد واطئ الكلفة لتفاعل الترانساسترة لتحويل زيت الخردل الهندي الى ديزل حيوي. يعتبر استخدام هكذا عامل مساعد واطئ الكلفة عامل مهم في جعل انتاج الديزل الحيوي منافس لوقود الديزل من الاصل النفطي. إن حركية التفاعل المحفز بواسطة العامل المساعد (Hydroxyapatite) تم دراستها بظروف متوسطة ( درجة حرارة 60 م, نسبة الايثانول الى الزيت 20:1 وكمية العامل المساعد 18% بالاعتماد على وزن الزيت). نماذج العوامل المساعدة تم دراسة خصائصها باستخدام تقنيات (XRD, FTIR, BET surface area). الدراسة الحالية بينت إن عملية (Transesterification) تتضمن مرحلة ابتدائية محددة بانتقال الكتلة لل (TG) ثم مرحلة سريعة وأخيرا مرحلة محددة بسرعة التفاعل الكيماوي. إن تحديد انتقال المادة لل (TG) كان سببه قلة توفر المساحة النوعية الفعالة للعامل المساعد نتيجة الامتزاز العالي للميثانول على سطح العامل المساعد. انتقال المادة لل (TG) وسرعة التفاعل الكيماوي كلاهما ازداد مع زيادة كمية العامل المساعد. الإستراتيجية المتبعة لنمذجة العملية تأخذ بنظر الاعتبار تأثير ظروف الخلط على عملية ال (Transesterification).

## **1. INTRODUCTION**

The depletion of fossil fuels in the near future and the increasing environmental impact have stimulated the alternative sources for fossil fuel development. advanced research and development on sustainable energy are important due to concerns over climate change and energy security. Biodiesel has considerable production potential as a renewable source of energy. The conventional processes use soluble alkali catalysts that contaminate the biodiesel and glycerol products, and present separation problems. An efficient and clean process is crucial for large scale commercial production. Solid catalysts have the potential to eliminate these problems[1]. Currently, transesterification reaction using basic catalysts is the most extended process to produce biodiesel. Metal oxides are the basic heterogeneous catalysts group most studied. There are several metal oxides that have been studied in bibliography: calcium oxide, magnesium oxide, strontium oxide, mixed oxides and hydroxalites[2].

The kinetics of catalyzed transesterification reaction has been studied previously in some studies. The triolein transesterification catalyzed by MgO was simulated by a three-step Eley-Rideal type of mechanism with the methanol adsorption on the catalyst active sites as the rate determining step[3]. The kinetics of soybean oil transesterification at high temperatures using metal oxide as a catalyst was described by a simple first-order kinetic model with respect to TG [4] or methanol [5]. The order of the CaO- and Ca(OH)<sub>2</sub>- catalyzed transesterification with respect to TG changed from zero to one with the reaction progress[6]. The Hydroxyapatite was found an efficient catalyst for biodiesel production from peanut and rapeseed oils in our previous study [7]. To the best of our knowledge there are no previous studies on the kinetic of hydroxyapatite-catalyzed transesterification reaction. In the present work the HAP- catalyzed transesterification of mustard oil was studied at the molar ratio of methanol to oil of 20:1 and 60°C. The transesterification was catalyzed by hydroxyapatite present in the range from 2% to 18% (based on the oil weight).

The present paper provides a kinetic study of HAP- catalyzed transesterification reaction carried out to check the process mechanism and report a simple model for the transesterification process kinetics which did not require complex computations.

## **2. EXPERIMENTAL**

### **2.1 Materials and catalyst preparation**

Mustard oil was purchased from local markets. Methanol, phosphoric acid were supplied from Fisher Scientific, India. Methyl ester, triolein were obtained from Sigma-Aldrich, Germany. All chemicals used were analytical reagents. Bones of goat animal were obtained from slaughter waste. Firstly, the bones were crushed into small chips and rinsed several times with hot water to remove impurities and undesirable materials. Subsequently, the clean bone chips were dried at 378 K for 24 h in a hot air oven. Then, the bone chips were grounded to fine powdered and subjected to additional drying at the same above conditions. After that, the fine bone powder was calcined in the muffle furnace at 900°C for 2 h under static air. Finally, the catalyst powders were stored in dark, well closed, glass bottle in a desiccator that contains calcium chloride and potassium hydroxide pellets.

### **2.2 Catalyst Characterizations**

The crystalline phases of calcined catalyst samples were analyzed by X-ray diffraction (XRD). The samples were characterized by N<sub>2</sub> adsorption-desorption (Micromeritics, ASAP 2020) for their BET surface area, pore volume and pore size. FTIR spectra were obtained with FTIR (Thermo-Nicolet 5700 model). The spectra were obtained in the 500–4000 cm<sup>-1</sup> region, with a resolution of 4 cm<sup>-1</sup>. Averages of 32 scans were recorded. The mean catalyst particle diameter was calculated from the mean particle perimeter which was determined microphotographically. HAP powder (0.025 g) was suspended in

paraffin oil (1 g) by means of a vortex agitator for 3 minutes. The microphotography was taken by a microscope equipped with a digital camera (Motic Digital Microscope; magnification: 400 times).

### 2.3 Experimental setup

The transesterification reaction was carried out in a batch reactor. A 500 mL three necked round bottom glass flask was used. It had provisions for a water-cooled condenser, thermometer, and mechanical stirrer. The flask was kept inside a water bath with thermostat which maintained the temperature at the desired level. The reaction mixture was stirred at 600, 800, and 1000 rpm for all test runs. The Photograph of the experimental set up is given in the **fig. 1**

### 2.4 Transesterification

The oils were heated at 378 K for 1 h in N<sub>2</sub>-purge to evaporate water and other volatile impurities. Heated oils were allowed to cool to room temperature. Subsequently, a mixture of methanol and catalyst at a designated amount was added to the oil. Each experiment was allowed to continue for a set period of time. The reaction mixture was allowed to cool down and equilibrate which resulted in separation of two layers. The upper layer consisted of methyl esters (biodiesel) and unconverted triglycerides. The lower layer contained glycerol, excess methanol, catalyst and any soap formed during the reaction and possibly some entrained methyl esters. After separation of the two layers by sedimentation the upper methyl esters layer was dried at 378 K for 4 h to remove water content from biodiesel layer. The catalyst was separated from lower layer by centrifugation and filtration.

### 2.5 Testing of vegetable oil and biodiesel (methyl esters) properties

In the present work, vegetable oil and methyl esters (biodiesel) were analyzed by FTIR (Thermo-Nicolet 5700 model). The spectra were obtained in the 500–4000 cm<sup>-1</sup> region, with a resolution of 4 cm<sup>-1</sup>. Averages of 32 scans were recorded using a multi bounce ATR. The method developed by Giuliano et al.[8] was used for quantitative analysis. The height of absorbance band at wave number 1741 cm<sup>-1</sup> was used to calculate the concentration of ester in the biodiesel layer. A calibration curve was obtained by measuring the height of the 1741 cm<sup>-1</sup> bands for samples of ester and oil of known compositions (methyl ester and triolein). The composition of the reaction mixture samples was determined by FTIR. **Figure 2** shows the FTIR spectra of produced biodiesel.

From the content of TG (in %) in the Biodiesel/oil fraction of the reaction mixture, the conversion degree of TG was calculated using the following equation (eq.(1)):

$$x_A = 1 - TG/TG_o \tag{1}$$

where  $TG_o$  is the initial percentage of TG in the Biodiesel/oil fraction.

The acid, saponification and iodine values were determined by the AOCS official methods [9]. The density and viscosity were measured at 20°C using a pycnometer and a rotational viscometer. **Table 1** shows the properties of mustard oil.

## 3. THEORY

The mustard oil transesterification reaction can be expressed by the following equation (eq. (2)):



where T is TG, M is methanol, B is fatty acid methyl esters (FAME) and G is glycerol. In the presence of heterogeneous catalysts, the transesterification reaction is very complex because the reaction mixture is a three-phase system (oil-methanol-catalyst). Besides transesterification, some side reactions occur too, such as saponification of glycerides and methyl esters, as well as neutralization of free fatty acids by an alkaline catalyst.

The kinetic model is derived by proposing heterogeneous reaction mechanism steps and using the following assumptions [10]:

1. The proposed HAP-catalyzed transesterification reaction mechanism is shown in the **fig. 3**.
2. The reaction mixture is perfectly mixed.
3. Methanol adsorption follows pseudo-first order kinetics.
4. The conversion of TG follows the pseudo-first order reaction kinetic. The supercritical and subcritical transesterification reaction of soybean oil with nano-MgO was described by the pseudo-first order reaction kinetics [11].
5. In the initial reaction period, the glyceride mass transfer rate towards the catalyst surface active sites can influence the overall process rate. The glyceride adsorption rate on the catalyst surface is determined by the glyceride mass transfer rate towards the catalyst surface active sites.
6. The internal diffusion rate does not influence the rate of the transesterification reaction.
7. The overall process rate is limited by the rate of the reaction between a methoxide ion and TG in the later reaction period.
8. The overall process rate does not limited by adsorption rate of transesterification products from the catalyst surface.
9. The neutralization of free fatty acids is ignorable and the saponification reaction is negligible.

The heterogeneous reactions occur in multiple complicated different steps. By comparing their rates, the rate-limiting step can be determined. Normally, the rate of the methanol adsorption on the catalyst active sites can be equated to the rate of the methanol concentration increase on the catalyst surface.

The mass balance of methanol on solid catalyst surface includes:

- ❖ the methanol mass transfer from the bulk of liquid towards the catalyst active sites.
- ❖ the methanol adsorption on catalytic sites.
- ❖ the rate of methanol depletion in a bulk phase (the methanol depletion reaction rate is equal to the FAME formation rate).

The reactant mass transfer coefficient depends on:

- ❖ the reaction mixture composition.
- ❖ the reaction temperature.
- ❖ the agitation speed.

The available active specific catalyst particle surface is dependent not only on the specific catalyst particle surface but also on the availability of the active sites for the reactant mass transfer. According to the assumptions (4), (5) and (7) the TG mass transfer rate is equal to the TG. With the reaction progress, the adsorbed methanol concentration decreases on the active catalyst surface and at the same time the fraction of the available active catalyst surface for TG adsorption and the volumetric TG mass transfer coefficient increase.

The chemical reaction between the adsorbed molecules of TG and methanol controls the overall process rate (eq. (3))[10]:

$$-\frac{dC_A}{dt} = k \cdot C_A \quad (3)$$

The TG concentration is related to the conversion degree of TG,  $x_A$  as follows (eq. (4)):

$$C_A = C_{A0}(1 - x_A) \quad (4)$$

Then:

$$\frac{dx_A}{dt} = k(1 - x_A) \quad (5)$$

Upon integration, the following equation is obtained:

$$-\ln(1 - x_A) = kt + C \quad (6)$$

where  $C$  is the integration constant. Thus, both the mass transfer and the reaction rate follow the first order kinetics with a different rate constant ( $k_{app}=k_{mt,A}$  and  $k_{app}=k$ , respectively).

## 4. RESULTS AND DISCUSSION

### 4.1 Catalyst Characterizations

It is seen in the **fig. 4** that the XRD pattern of calcined animal bone at 900 °C shows sharper peaks, indicating better crystallinity. The average HAP catalyst particle size was 2.8 μm. The peak positions for hydroxyapatite (HAP) are in good agreement with the JCPDS (09-0432) having lattice parameters  $a = b = 0.942$  nm,  $c = 0.688$  nm, and no pattern indicating the presence of impurities was observed when bone was calcined at 900 °C. This confirms the hexagonal structure of standard HAP. The FTIR patterns of fresh and calcined Bone at 800 °C, 900 °C and 1000 °C are presented in **fig. 5**. The presences of  $\text{OH}^{-1}$  and  $\text{PO}_4^{-3}$  functional groups were confirmed by FTIR spectra. The intensity of the  $\text{OH}^{-1}$  stretching band is moderate in the spectra of fresh and calcined animal bone at 800 °C and 1000 °C and high in the spectra of calcined animal bone at 900 °C. It is seen from **fig. 5** that the carbonate is removed at 900 °C. The BET surface area of catalyst synthesized from waste animal bone at 900 °C was  $90.65 \text{ m}^2\text{g}^{-1}$ . This is higher than that of other two catalysts calcined at 800 °C and 1000 °C.

### 4.2 Biodiesel yield analysis

**Figure 6** shows the progress of the mustard oil transesterification reaction. The temperature was 60 °C, the catalyst was 18 wt % HAP, and the methanol/oil molar ratio was 20:1. The change of TG concentration with time was showing sigmoidal shape with three stages existed. In the initial stage of the reaction, production of FAME was slow. Then, the rate was rapid in the medium stage and finally in the last stage reached equilibrium in about 240 min. The increase in FAME concentration was associated by an increase in glycerol concentration as it was liberated from TG molecules. However, the relative proportion of GL produced was not always the same as that of the esters produced. This is due to intermediate products such as DG and MG. This type of kinetics has already been observed for the homogeneously base-catalyzed transesterification [12-15]. This shape might be partially associated with the increasing solubility of methanol in the oil-FAME phase with the formation of FAME [16]. In all the experiments, the increase of the FAME concentration followed the decrease of the TG

concentration. The concentrations of intermediate products, monoglycerides (MG) and diglycerides (DG), increased at the beginning of the reaction achieving their maximum, then decreased and finally stayed nearly constant.

### 4.3 Mass transfer controlled region

Before checking the kinetic model, the intra particle diffusion and external liquid-solid mass transfer limitations both were checked. The diffusion of the reactants from the surface to the active sites within the catalyst particles controls the reaction rate if the internal mass transfer limitations exist. Firstly the effectiveness factor must be estimated, which can be estimated from the Thiele modulus. The Thiele modulus for a spherical particle is given as the following equation [17]:

$$Th = \frac{R_p}{3} \sqrt{\frac{k}{D_{eff}}} \quad (7)$$

where  $R_p$  is the particle radius;  $k$  is the pseudo-first order reaction rate constant and  $D_{eff}$  is the effective diffusion coefficient. In the present work, the estimated values of the average particle size and the pseudo-first-order reaction rate constant for the catalyst amount of 18% were determined to be  $2.8 \mu m$  and  $0.060 \text{ min}^{-1}$ , respectively. From the molecular diffusion coefficient and the porosity and the tortuosity of the catalyst particle, the effective diffusion coefficient can be determined. Using the Wilke and Chang correlation [18], the estimated values of the molecular diffusion coefficient of TG through methanol and TG were  $6.2 \times 10^{-6}$  and  $4.3 \times 10^{-7} \text{ m}^2/\text{s}$ , respectively. Thiele modulus value was calculated to be 0.01 or 0.038 for the diffusion of TG through methanol and TG, respectively. Because of the small Thiele modulus values (i.e.  $Th < 0.4$ ), that mean, the effectiveness factor is equal to 1 and the internal diffusion resistance was negligible, and verifying the assumption (8).

The reaction rate is controlled by the mass transfer of the reactant from the bulk liquid phase to the surface of the catalyst particles if external liquid-solid mass transfer limitations exist. By studying the effect of mixing speed on the reaction rate under the same reaction conditions, the presence of external mass transfer limitation was concluded experimentally. The reaction was carried out at 600, 800 and 1000 rpm. The variation of TG conversion degree with time is shown in **Fig. 7** and indicates that both the reaction rate and the final reactant conversion degree were not affected by the mixing speed, signifying the absence of external mass transfer resistance. The phenomena that occurred in the initial region of the HAP- transesterification of mustard oil have been already observed in the reaction catalyzed by  $\text{Ca}(\text{OH})_2$  [19]. In the beginning of the reaction, the methanol molecules occupied the catalyst surface active sites which reduced the available active specific catalyst surface area. As a result of that, the volumetric TG mass transfer coefficient was small (due to very small  $\theta$ ) and the overall reaction rate was limited by the TG mass transfer rate (the assumption 5). The methanol drops were broken down and stabilized by surface active compounds formed in the reaction. The occurrence of the catalyst particle path through the surface of the dispersed methanol drops was increased due to the drop breakage process growth. The importance of the external mass transfer limitation was reduced to nothing with the progress of transesterification process as the available active specific catalyst surface and the TG mass transfer rate increased.

### 4.4 Kinetics of reaction

The Boltzman function were used to define the sigmoidal fits of the experimental data on the methanol and FAME concentrations in the liquid phase. The methanol concentration change with time on the

catalyst surface was calculated from the rates of FAME and the methanol concentration changes  $dC_B/dt$  and  $dC_M/dt$ , respectively in the liquid phase.

In **Fig.8** the change of methanol concentration adsorbed on the catalyst surface active sites was plotted against the reaction time. It can be concluded that the HAP catalyst was saturated with methanol at the initial period. The decrease in the concentration of the adsorbed methanol could be expected due to the addition of oil to the catalyst-methanol mixture. Also due to glyceride mass transfer limitations, in the initial reaction period  $dQ/dt \approx 0$ , the chemical reaction was very slow. After that, the adsorbed methanol concentration was decreased with reaction time and  $dQ/dt < 0$ . Because of the high adsorbed methanol concentration on the catalyst surface, the chemical reaction was faster than the methanol adsorption, but did not limit the overall process. The kinetic regime was changed based on the  $dQ/dt$  change in this period. The plot of  $dQ/dt$  with time was changed in three periods, Firstly decreasing period, secondly reaching minimum period and then finally increasing period. A slow chemical reaction rate was concluded in the initial decreasing period due to the slower adsorption of methanol molecules. In the second short period, the chemical reaction became faster due to the faster decreasing of methanol adsorption. It can be concluded that the kinetic regime start changing at the time when  $dQ/dt$  reached the minimum in the plot. Finally, when  $dQ/dt > 0$ , it can be concluded that the methanol adsorption rate was faster than the chemical reaction. Confirming the assumption (3), it was found that the mass transfer and the adsorption of methanol did not limit the transesterification reaction at all. At the end of the reaction, Mathematically  $dQ/dt = 0$ , i.e.  $Q = const$ .

In **Fig.9** the change of  $-\ln(1-x_A)$  was plotted against time for the transesterification reaction carried out at different catalytic conditions. It can be seen from **Fig. 9** that the overall process was limited by TG mass transfer ( $k_{mt,A} = const$ ) and by chemical reaction, respectively. The increase of TG mass transfer due to the increase of the active catalyst surface in the presence of higher catalyst amounts was concluded. As an explanation, Increasing the catalyst amount decrease the period where TG mass transfer limited the overall process rate. After a short period of time, the nonlinearity of  $-\ln(1-x_A)$  plot can be seen due to the increase in volumetric TG mass transfer coefficient with the increase of the available active catalyst surface. At the minimum  $dQ/dt$ , the volumetric TG mass transfer coefficient became higher than the pseudo-first order reaction rate constant. Therefore in the final reaction period, the reaction controlled the overall process rate. From the slope of relation  $-\ln(1-x_A)$  with time in the final process period, the pseudo first order reaction rate constant was calculated.

It can be concluded that the lumped parameter  $k_{s,A} \cdot \theta_o \cdot a_m$  as well as the value of  $\theta_o$  in the initial period of the transesterification reaction were independent of the catalyst amount in the reaction system because the volumetric TG mass transfer coefficient increased proportionally with the catalyst amount as seen in **Fig. 10**. Practically, it was found that the pseudo-first order reaction rate constant did not depend on the catalyst amount with the value of  $0.080 \text{ min}^{-1}$ .

when the TG mass transfer rate became equal to the rate of the reaction, then at this time [10]:

$$k_{s,A} \cdot \theta_1 \cdot a_m \frac{m_{HA}}{V} = k \tag{8}$$

where  $\theta_1$  is the fraction of the available active specific surface when the chemical reaction began to control the overall process rate. Now, by dividing Eq. (8) by  $k_{s,A} \cdot \theta_o \cdot a_m \frac{m_{HA}}{V}$ , we can obtain

$$\frac{\theta_1}{\theta_o} = \frac{k}{k_{mt,A}} \tag{9}$$



During the middle period of the transesterification reaction and for a specified catalyst amount, The fraction of the available active specific surface was increased. Although, the ratio  $\theta_1/\theta_0$  decreased with increasing the catalyst mentioned amount (**Fig. 10**).

#### 4.5 Modeling of reaction kinetics

The decay of TG conversion degree in time was sigmoidally fitted. It was found that the relative deviations of calculated (based on the sigmoidal fit) and experimental TG conversion degree were  $\pm 10.3\%$ ,  $\pm 1.4\%$ ,  $\pm 1.8.0\%$  and  $2.1\%$  at HAP amounts of 2%, 8%, 12% and 18%, respectively. Based on the proposed kinetic model, the TG conversion degree was calculated from the following equations[19]:

- for TG mass transfer controlled regime ( $k_{mt,A} = \text{const}$ ):

$$x_A = 1 - \exp(-k_{mt,A}t) \quad (10)$$

- for chemical reaction controlled regime:

$$x_A = 1 - \exp(-kt - C) \quad (11)$$

The kinetic model was also compared with the experiment based on the changes of the molar concentrations of TG and FAME. **Figure 11** shows that the kinetic model was fitted well with the experimental data in the initial and later reaction periods but not in the period when FAME formation rate rapidly increased.

## 5. CONCLUSIONS

1. Compared to catalysts calcined at other temperatures, the bone catalysts calcined at  $900^\circ\text{C}$  shows low crystallite size and higher BET surface area .
2. The optimum conditions for maximum biodiesel yield were (20:1 molar ratio of methanol to oil, addition of 18 wt% of bone catalyst (calcined at  $900^\circ\text{C}$ , 2 hr),  $60^\circ\text{C}$  reaction temperature and reaction time of 4 hrs).
3. A simple model was used to study the kinetics of HAP heterogeneously catalyzed transesterification reaction.
4. The activity of HAP catalyst effect the transesterification reaction between methanol and glyceride molecules which adsorbed on the surface catalyst active sites.
5. The sigmoidal kinetics of the process was explained by TG mass transfer limitations in the initial region, followed by the chemical reaction controlled region in the latter period. The overall chemical reaction followed the pseudo-first order reaction kinetics.
6. The TG mass transfer limitation was caused by the low available active specific catalyst surface because of the high adsorbed methanol concentration.
7. The available active specific catalyst surface increased with the catalyst amount increase, thus the mass transfer resistance significantly decreased at higher catalyst amounts.

## REFERENCES

- [1] Enweremadu CC, Mbarawa MM. Technical aspects of production and analysis of biodiesel from used cooking oil – a review. *Renewable and Sustainable Energy Reviews* 2009;13:2205–24.
- [2] Borges M.E., Díaz L. Recent developments on heterogeneous catalysts for biodiesel production by oil esterification and transesterification reactions: A review. *Renewable and Sustainable Energy Reviews* 2012; 16: 2839– 2849.
- [3] Dossin, T.F., Reyniers, M.-F., Marin, G.B. Kinetics of heterogeneously MgO catalyzed transesterification. *Appl. Catal. B* 2006; 61, 35-45.
- [4] Wang, L., Yang, J.. Transesterification of soybean oil with nano-MgO or not in supercritical and subcritical methanol. *Fuel* 2007; 86L: 328-333.
- [5] Singh, A.K., Fernando, S.D.. Reaction kinetics of soybean oil transesterification using heterogeneous metal oxide catalysts. *Chem. Eng. Technol.* 2007; 30: 1716-1720.
- [6] Kouzu, M., Kasuno, T., Tajika, M., Sugimoto, Y., Yamanaka, S., Hidaka, J. Calcium oxide as a solid base catalyst for transesterification of soybean oil and its application to biodiesel production. *Fuel* 2008; 87: 2798-2806.
- [7] Jazie, A. A., Pramanik, H., & Sinha, A. S. K. Transesterification of peanut and rapeseed oils using waste of animal bone as cost effective catalyst. *Materials for Renewable and Sustainable Energy* 2013; 2(2): 1-10.
- [8] Giuliano F Zagonel, Patricio Peralta-Zamora, Luiz P Ramos. Multivariate monitoring of soybean oil ethanolysis by FTIR. *Talanta* 2004;63:1021–1025.
- [9] AOCS. Official and tentative methods. Chicago: American Oil Chemists Society; 1980.
- [10] Smith, J.M. *Chemical Engineering Kinetics*. 3rd edition, McGraw-Hill International Book Company, 1981.
- [11] Wang L, Yang J. Transesterification of soybean oil with nano-MgO or not in supercritical and subcritical methanol. *Fuel* 2007; 86:328-33.
- [12] Jazie, A. A., Sinha, A. S. K., & Pramanik, H. Optimization of Biodiesel Production from Peanut and Rapeseed Oils Using Response Surface Methodology. *International Journal of biomass & renewables*, 2012; 1(2): 9-18.
- [13] Nouredini H, Zhu D. Kinetics of transesterification of soybean oil. *J Am Oil Chem Soc* 1997;74:1457-63.
- [14] Stamenkovic´ OS, Todorovic´ ZB, Lazic´ ML, Veljkovic´ VB, Skala DU. Kinetics of sunflower oil methanolysis at low temperatures. *BioresTechnol* 2008;99:1131-40.

- [15] Vicente G, Martinez M, Aracil J, Esteban A. Kinetics of sunflower oil methanolysis. *IndEngChem Res* 2005;44:5447-54.
- [16] Stamenkovic´ OS, Lazic´ ML, Todorovic´ ZB, Veljkovic´ VB, Skala DU. The effect of agitation intensity on alkali-catalyzed methanolysis of sunflower oil. *BioresTechnol* 2007;98:2688-99.
- [17] Levenspiel O. *Chemical reaction engineering*. 3rd ed. New York: John Wiley and Sons; 1999.
- [18] Poling, B.E., Prausnitz, J.M., O´ Connell, J.P. *The Properties of Gases and Liquids*, fifth ed. McGraw-Hill, New York;2004.
- [19] Stamenkovic´ Olivera S., Veljkovic´ Vlada B., Todorovic´ Zoran B., Lazic´ Miodrag L., Bankovic´ -Ilic´ Ivana B., SkalaDejan U. Modeling the kinetics of calcium hydroxide catalyzed methanolysis of sunflower oil *Bioresource Technology* 2010;101: 4423–4430

**Table 1:** The properties of mustard oil.

Acid value (mg KOH/g)	0.23
Saponification value (mg KOH/g)	175
Iodine value (g J <sub>2</sub> /100 g)	112
Density (kg/m <sup>3</sup> ) at 20°C	910
Viscosity (mPa s) at 20°C	88



**Figure 1:** Photograph of experimental setup.

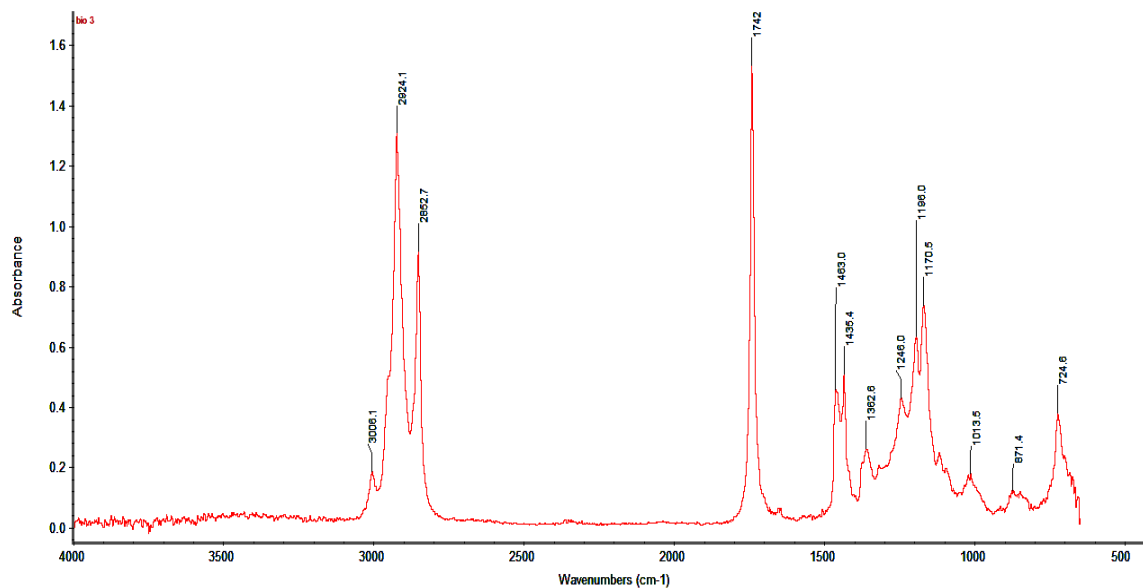


**Figure 2:** FTIR spectra of biodiesel product.

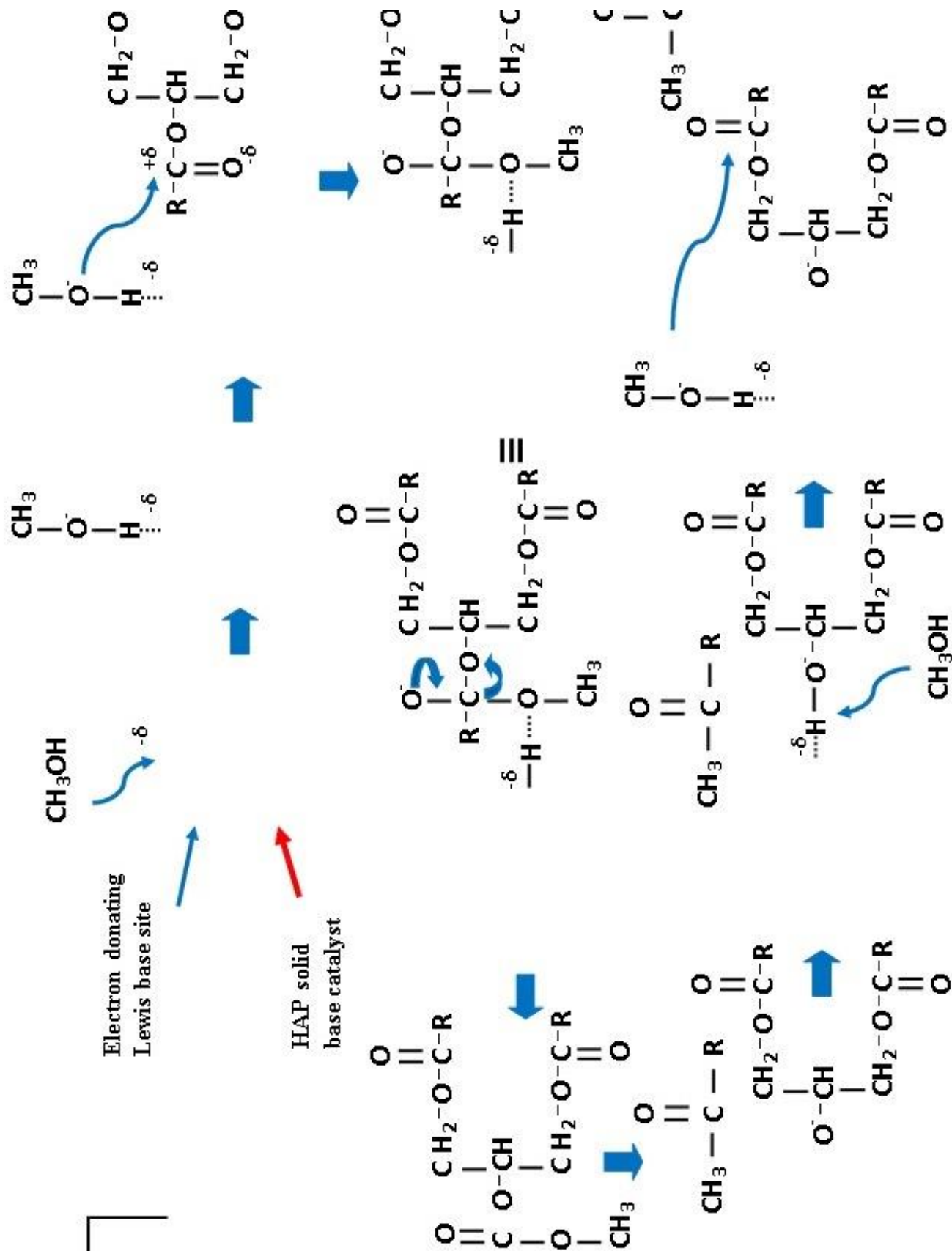
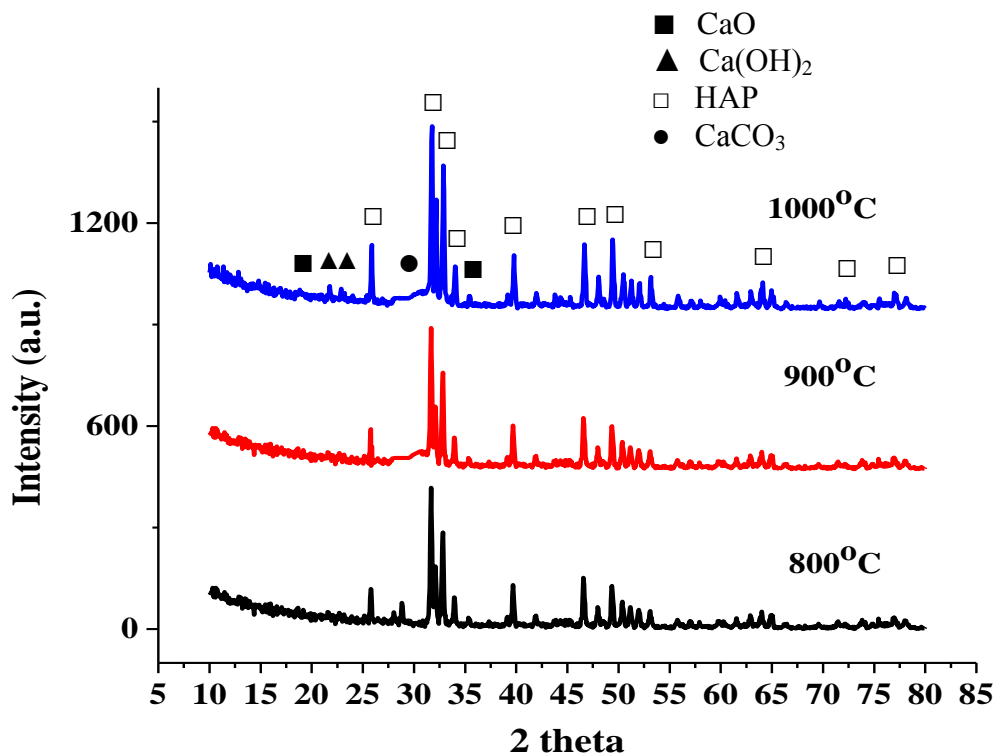
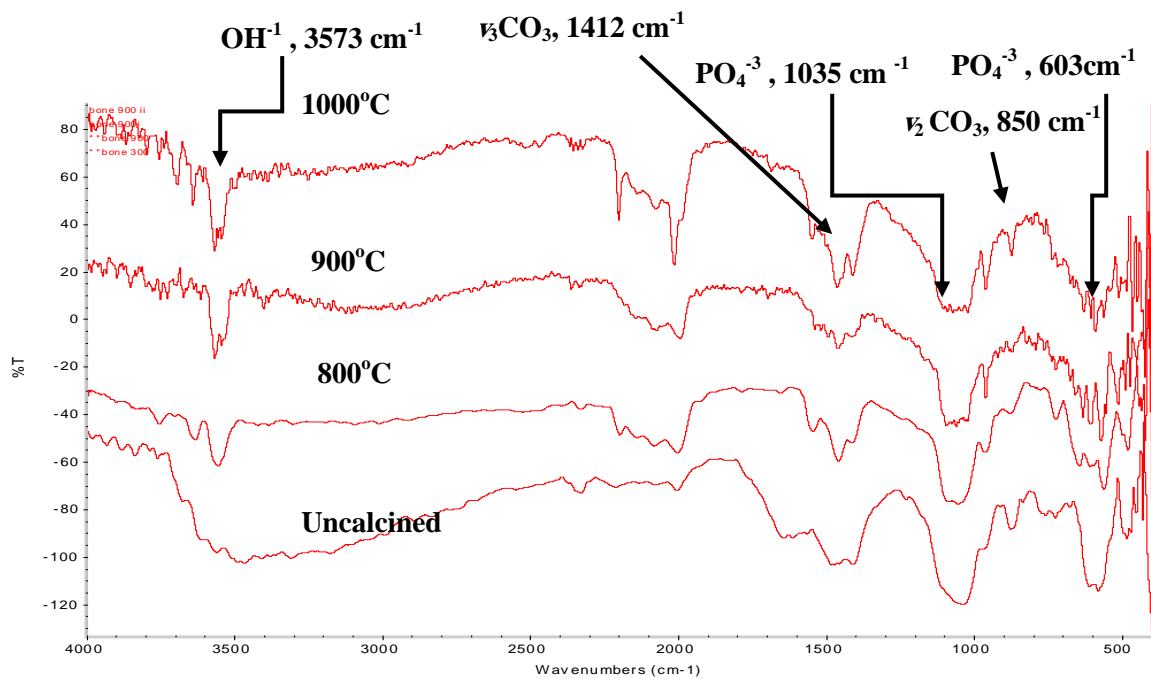


Fig. 3 The mechanism for hydroxyapatite (Ca<sub>10</sub>(PO<sub>4</sub>)<sub>6</sub>(OH)<sub>2</sub>) catalysis in transesterification reaction.



**Figure 4:** XRD of the calcined bone catalyst at 800 °C, 900 °C and 1000 °C, respectively.



**Figure 5:** FTIR spectra of fresh bone and calcined bone samples at 800 °C, 900 °C and 1000 °C , respectively

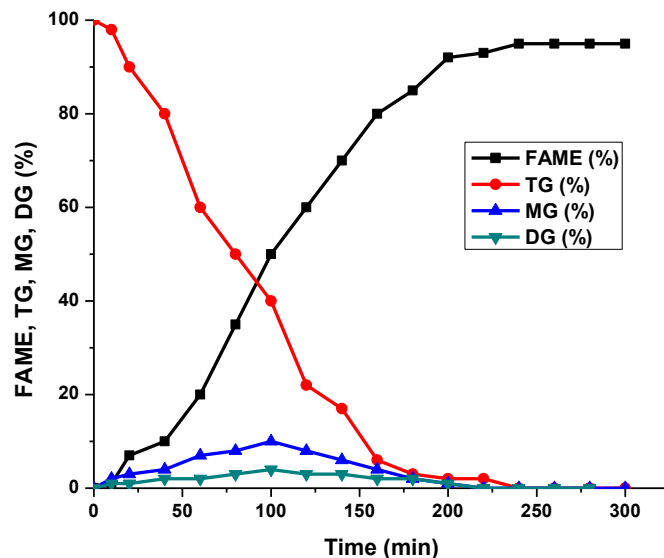


**Figure 6:** The variations of the reaction mixture composition with the progress of HAP-catalyzed transesterification of mustard oil (catalyst amount, based on the oil weight, %: 18; average catalyst particle size,  $\mu\text{m}$ : 2.8).

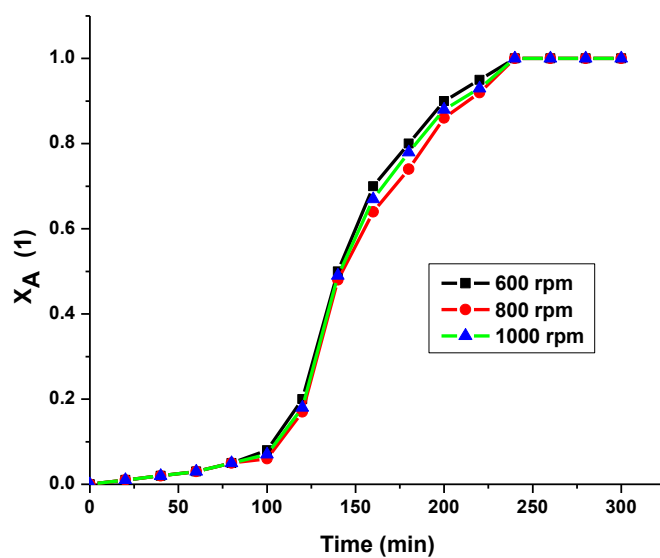


**Figure 7:** The influence of the agitation speed on the conversion degree of TG ( $60^{\circ}\text{C}$ ;methanol to oil ratio: 20:1; 18% of the catalyst based on the oil amount).

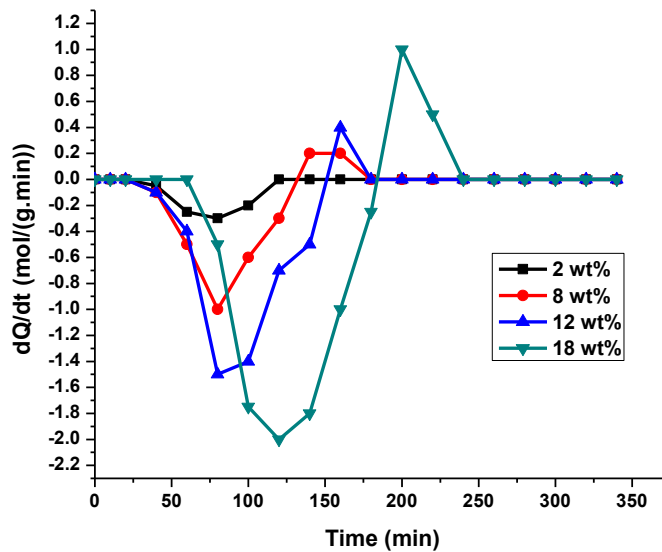


**Figure 8:** The rate of the adsorbed methanol concentration variations on the catalyst active sites with the progress of HAP-catalyzed transesterification (catalyst amount, based on the oil weight,%; average catalyst particle size,  $\mu\text{m}$ : 2.8).

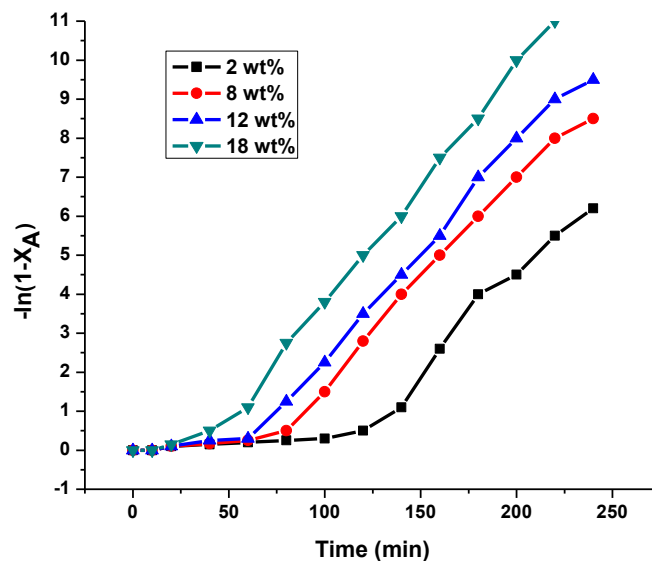


**Figure 9:** Dependence  $-\ln(1-x_A)$  versus  $t$  during HAP-catalyzed transesterification (catalyst amount, based on the oil weight,%; average catalyst particle size,  $\mu\text{m}$ : 2.8).



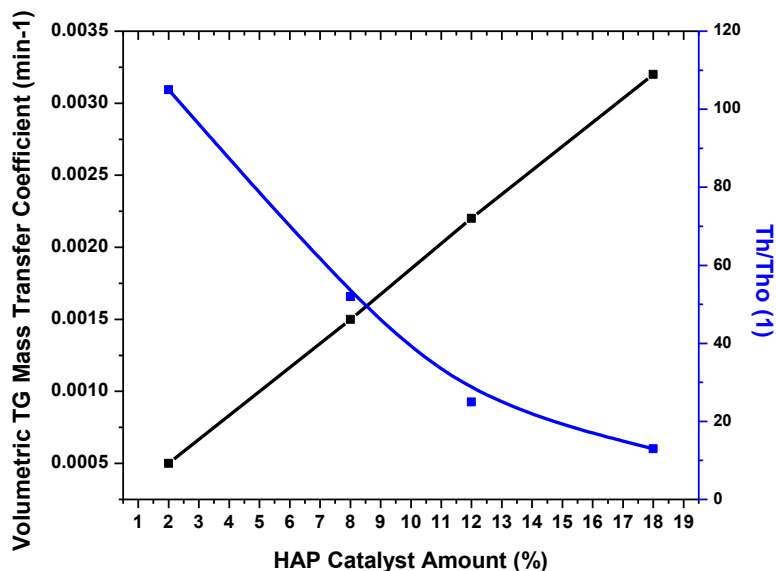


**Figure 10:** The volumetric TG mass transfer coefficient and the ratio  $\theta_1/\theta_2$  at various catalyst amounts (average catalyst particle size,  $\mu\text{m}$ : 2.8).

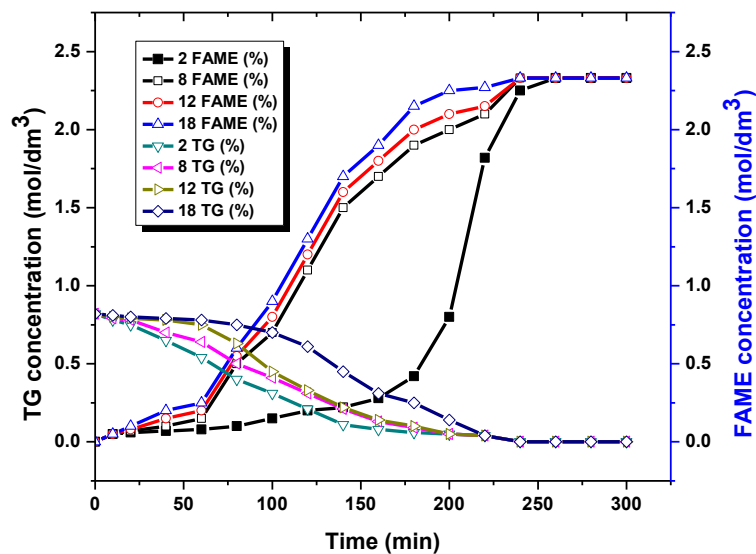


**Figure 11:** The comparison of TG and FAME concentrations calculated by the kinetic model (mass transfer, chemical reaction) with the experimental data during HAP-catalyzed transesterification (catalyst amount, based on the oil weight, %; average catalyst particle size,  $\mu\text{m}$ : 2.8).